Nonreciprocal GaAs Phase-Shifters and Isolators for Millimetric and Sub-Millimetric Wavelengths

V. H. Mok and L. E. Davis

The Electromagnetics Centre, Dept. of Electrical Eng. & Electronics, University of Manchester Institute of Science and Technology (UMIST), P O Box 88, Manchester M60 1QD, U.K.

***Abstract*—Two new nonreciprocal waveguiding structures — a grounded-dielectric/semiconductor slab and a grounded-semiconductor/dielectric slab have been investigated analytically and numerically. The results demonstrate nonreciprocal behavior and the potential for the design of phase shifters and isolators in millimetric and sub-millimetric wavelengths region. Dispersion diagrams are plotted to show the wave behavior for both structures.**

I. Introduction

The theory of surface magnetoplasmons in two semi-infinite media in which one of the media is semiconductor or plasma is already available [1]-[4]. Talisa and Bolle [5, 6] have studied surface magnetoplasmons with device applications in mind.

In this paper we report, for the first time, two new nonreciprocal structures – a grounded dielectric slab with a semiconducting top layer and a grounded semiconductor slab with a dielectric top layer. The materials assumed for this modeling are a low loss dielectric with $\varepsilon_d = 10$ and an *n*-type GaAs. The semiconductor is assumed to be lossless (collision frequency, $\nu_c = 0$). A uniform external magnetic flux density B_0 is applied in the y direction (parallel to the slab surfaces) and perpendicular to the direction of propagation. Dispersion ($\beta - f$) diagrams are plotted to show the forward and reverse wave behavior for both structures and their similarities and differences are discussed. The design of components such as phase shifters and isolators for millimeter and sub-millimeter wavelengths looks promising for both proposed structures. The nonreciprocal behavior observed will be explained in detail.

II. Theory

An *n*-type GaAs has been taken as the semiconductor material, with a carrier concentration $N_e \approx 2\times10^{14}$ cm^{-3} [7]. The applied flux density $B_0 = 0.15$T, and this value of B_0 is also used in [5, 6]. With the material cooled at 77K, mobilities in the order of 2.1×10^5 cm^{2}Vs^{-1} can be obtained and these parameters yield a plasma frequency, $\omega_p = 0.85\times10^{12}$ rad/s and a cyclotron frequency, $\omega_c = 0.39\times10^{12}$ rad/s. The electron interaction with the applied electromagnetic field in a semiconductor material is well described by the Drude-Zener model [8]. Using this model, the tensor permittivity with magnetic field in y direction can be written in the form

$$[\varepsilon] = \begin{bmatrix} \xi & 0 & -j\eta \\ 0 & \zeta & 0 \\ +j\eta & 0 & \xi \end{bmatrix} \quad (1)$$

where ξ, η and ζ are highly frequency dependent and are defined in [8, 9]

With a transverse magnetic bias and TM mode propagation, the effective relative permittivity, ε_{eff} is defined by (2) and Fig. 1 shows a plot of ε_{eff} as a function of frequency for *n*-type GaAs at 77K.

$$\varepsilon_{eff} = \frac{\xi^2 - \eta^2}{\xi} \quad (2)$$

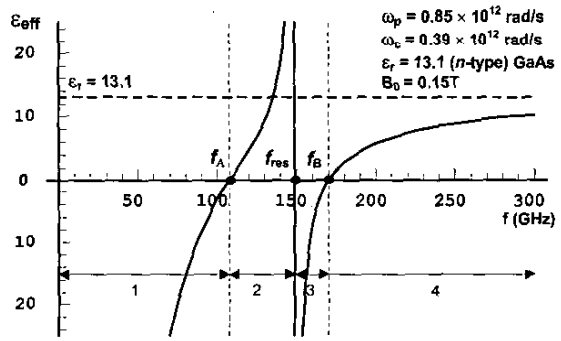

Fig. 1. Effective relative permittivity as a function of frequency for (*n*-type) GaAs at 77K. The material is assumed to be lossless.

The semiconductor effective relative permittivity is negative in two frequency regions, i.e., for $0 < f < f_A$ (region 1) and $f_{res} < f < f_B$ (region 3) and is positive for $f_A < f < f_{res}$ (region 2) and $f > f_B$ (region 4). Thus magnetized

0-7803-7695-1/03/$17.00 © 2003 IEEE

semiconductor offers a greater wealth of modes compared to ferrite material and a higher frequency range of operation. The important frequencies are denoted by f_A, f_{res} and f_B in Fig. 1.

A. Grounded-dielectric/semiconductor slab

At frequencies where $\varepsilon_{eff} \leq 0$, the structure in Fig. 2 can be used as a waveguide where the field is more concentrated in the dielectric slab of thickness h between the ground plane and the semiconductor. The semiconductor is assumed to be lossless ($\nu_c = 0$). An external magnetic flux density B_0 is perpendicular to the direction of wave propagation.

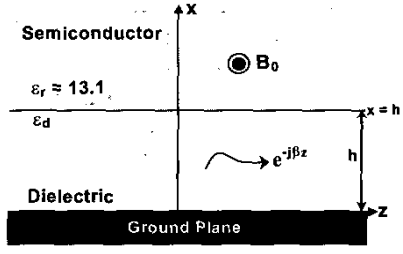

Fig. 2. Geometry of grounded-dielectric/semiconductor slab.

Only TM modes (H_y, E_x, and E_z) are considered in this analysis. Using Maxwell's equations and the boundary conditions, it can be shown that

$$\begin{aligned} k_r^2 &= \beta^2 - \varepsilon_{eff} k_0^2 \quad \text{for semiconductor} \\ k_d^2 &= \varepsilon_d k_0^2 - \beta^2 \quad \text{for dielectric} \end{aligned} \tag{3}$$

and the dispersion relation can be shown to be

$$\varepsilon_{eff} k_d \tan(k_d h) - \varepsilon_d (k_r \pm \gamma\beta) = 0 \tag{4}$$

where γ is the gyrotropic ratio defined as (η/ξ).

B. Grounded-semiconductor/dielectric slab

At frequencies where $\varepsilon_{eff} > 0$, the structure in Fig. 3 can be used as a waveguide where the field is more concentrated in the semiconductor slab of thickness h between the ground plane and the dielectric.

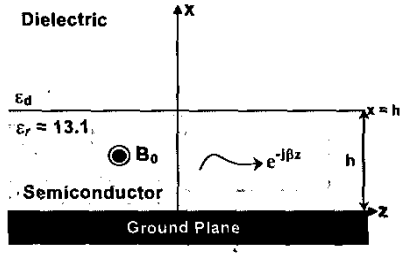

Fig. 3. Geometry of grounded-semiconductor/dielectric slab.

Using Maxwell's equations and the boundary conditions, it can be shown that

$$\begin{aligned} k_d^2 &= \beta^2 - \varepsilon_d k_0^2 \quad \text{for dielectric} \\ k_r^2 &= \varepsilon_{eff} k_0^2 - \beta^2 \quad \text{for semiconductor} \end{aligned} \tag{5}$$

and the dispersion relation can be shown to be

$$\varepsilon_d k_r \tan(k_r h) - \varepsilon_{eff} k_d - \varepsilon_d (\pm\gamma\beta) = 0 \tag{6}$$

III. Dispersion Diagram—Grounded-Dielectric/Semiconductor Slab

We first study the case of the grounded-dielectric/semiconductor slab (Fig. 2) when $\varepsilon_d = 10$ and the semiconductor is cooled to 77K. The applied flux density is $B_0 = 0.15$T which corresponds to $\omega_c/\omega_p = 0.46$.

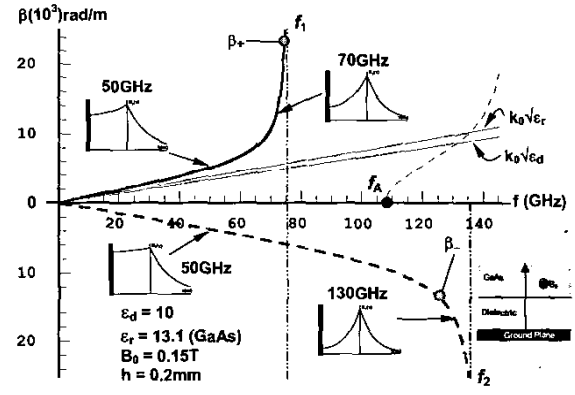

Fig. 4. Dispersion diagram of the grounded-dielectric/semiconductor (GaAs) slab in region 1 ($\varepsilon_{eff} \leq 0$). The applied magnetic flux density is $B_0 = 0.15$T.

In this summary, discussion is confined to frequency region 1, i.e., when $\varepsilon_{eff} \leq 0$. [Regions 2, 3 and 4 have been computed but are not shown for brevity.] Fig. 4 shows the dispersion diagram $(\beta - f)$ plot over the frequency range in region 1. Both the forward and reverse mode start from the origin, rise and asymptotically approach $\beta \to \infty$ as frequencies increased to f_1 = 75.45GHz and f_2 = 138.10GHz respectively. For $f_1 < f < f_2$ only a reverse wave exists over a bandwidth of 62.65GHz. This suggests the utilization of this spectral gap region for the design of nonreciprocal devices such as isolators.

Surface plasmon behavior can be observed in both the forward and reverse wave. The transverse magnetic field distribution $[H_y(x)]$ as function of x for both waves are illustrated in Fig. 4 (see insets). Selected frequencies were chosen to show the field variations for both waves. It can be seen that at 50GHz ($\varepsilon_{eff} < 0$) the field decays

transversely exponentially in the semiconductor region for both waves and it decays exponentially faster in the grounded-dielectric region for β_+ than β_-. It can be seen that the field for β_+ is bound more tightly to the interface and that $\beta_+ > \beta_-$. Surface plasmon behavior can be observed for β_+ at 70GHz and at 130GHz for β_- [solutions for β_+ do not exist at the higher frequency]. The nonreciprocal field displacement effect described above is similar to that in ferrite structures first discussed by Wiesbaum and Seidel [10], and semiconductor isolator and circulators based on this effect are envisaged. It is also noteworthy that β_- surface magnetoplasmons exists at frequencies above f_A, i.e. where $\varepsilon_{eff} > 0$.

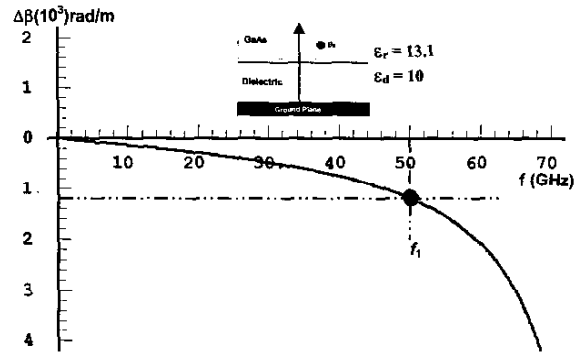

Fig. 5. Phase difference, ($\Delta\beta = \beta_- - \beta_+$) versus frequency for a grounded-dielectric/semiconductor slab. $\varepsilon_d = 10$, $\varepsilon_r = 13.1$ (*n*-type) GaAs and $B_0 = 0.15$T.

Fig. 5 shows the differential phase difference $\Delta\beta$ versus frequency for the grounded-dielectric/semiconductor slab described in Fig. 4. At frequency $f_1 = 50$GHz, $|\Delta\beta| = 1.2$ rad/mm = 68.75° rad/mm.

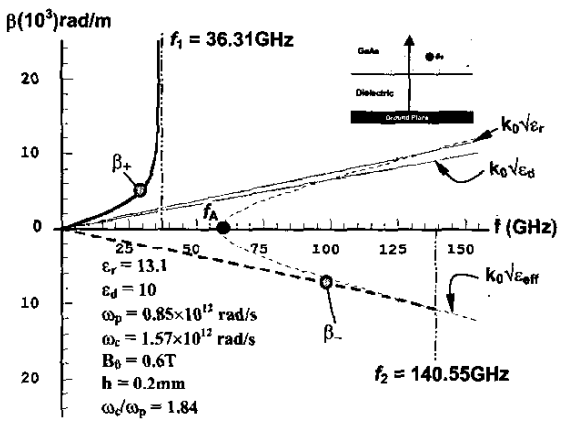

Fig. 6. Dispersion diagram of the grounded-dielectric/semiconductor slab when $B_0 = 0.6$T.

When the applied magnetic flux density, B_0 is increased to $B_0 = 0.6$T ($\omega_c/\omega_p = 1.85$) the dispersion curve changes to that shown in Fig. 6. The branch of the forward mode asymptotically approaches $\beta \to \infty$ at a lower frequency ($f_1 = 36.31$GHz) and the dispersion curve for the reverse mode terminates when it intersects the curve of the effective propagation constant, $k_0\sqrt{\varepsilon_{eff}}$ ($k_r = 0$) at $f_2 = 140.55$GHz. The bandwidth over which only the reverse wave exists has increased to 100GHz.

IV. Dispersion Diagram—Grounded-Semiconductor/Dielectric Slab

The dispersion diagram of the grounded-semiconductor/dielectric over the frequency range of regions 1 and 2 is shown in Fig. 7 (regions 3 and 4 not shown for brevity).

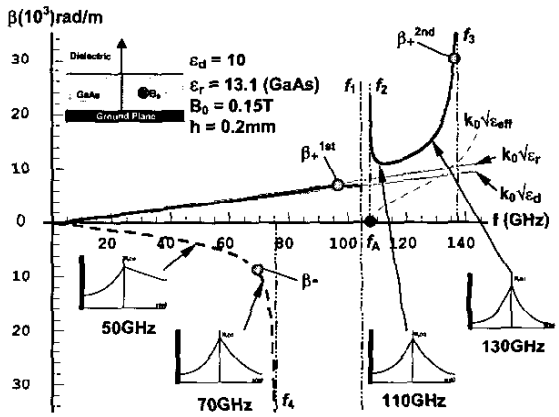

Fig. 7. Dispersion diagram of the grounded-semiconductor/dielectric slab in regions 1 ($\varepsilon_{eff} \le 0$) and 2 ($\varepsilon_{eff} > 0$). The applied magnetic flux density is $B_0 = 0.15$T.

The dispersion curve for the forward mode (β_+^{1st}), starts from the origin and terminates when the curve intersects the dispersion curve of $k_0\sqrt{\varepsilon_d}$ ($k_d = 0$) at $f_1 = 104.17$GHz. The curve for the second mode (β_+^{2nd}), starts from $f_2 = 107.80$GHz, falls and then rises and asymptotically approaches infinity at $f_3 = 138.10$GHz. For the reverse mode (β_-), the dispersion curve starts from the origin, rises and asymptotically approaches infinity at $f_4 = 75.50$GHz. This is similar to the behavior of the forward wave in Figs. 4 and 6, and this is because the semiconductor/dielectric interface has been inverted. It can be noted that only the forward wave exists in the frequency range $f_4 < f < f_1$ and $f_2 < f < f_3$ as shown in Fig. 7. Since the field is trapped in the semiconductor between the ground plane and the dielectric this structure can act as

a waveguide in region 1 ($\varepsilon_{eff} \leq 0$) for reverse wave β_- and in region 2 ($\varepsilon_{eff} > 0$) for forward wave β_+^{2nd}.

The transverse magnetic field distribution [$H_y(x)$] as function of x for both waves are shown in Fig. 7 (see insets). The branch corresponding to β_+^{1st} is of the little interest since the field is loosely bound at the interface (not shown). Only selected frequencies on the branches of the dispersion curve will be chosen to describe the behavior of the modes. At 50GHz and 70GHz for the reverse wave (β_-), the field behavior is similar to that of the forward wave shown in Fig. 4. For the forward wave (β_+^{2nd}), the surface plasmon behavior could be observed in the frequency range $f_2 < f < f_3$. Field distributions at 110GHz and 130GHz are shown in Fig. 7. The frequency range $f_2 < f < f_3$ could be utilized for designing isolators at sub-millimeter wavelengths since only the forward wave exists in this region. There is no mode corresponding to β_-^{2nd} between f_A and f_{res}.

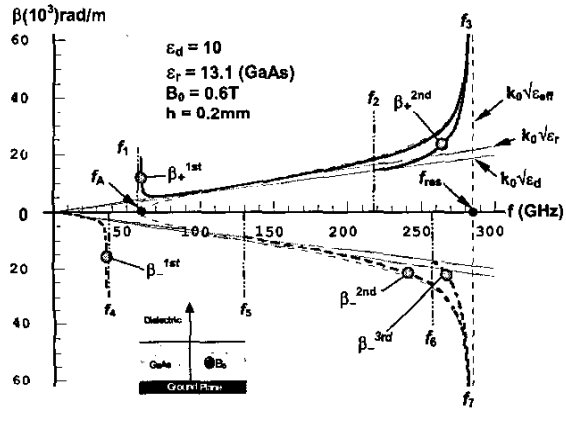

Fig. 8. Dispersion diagram of the grounded-semiconductor/dielectric slab when $B_0 = 0.6T$.

The dispersion curve of the grounded-semiconductor/dielectric when $B_0 = 0.6T$ is shown in Fig. 8. The bandwidth of the region 2 ($\varepsilon_{eff} > 0$) is increased and more modes were found. In particular, β_- modes exist in region 2 in contrast to their absence in Fig. 7. However, β_+ does not exist below f_1 (unlike Fig. 7). Only two modes each for forward wave (β_+^{1st} and β_+^{2nd}) and reverse wave (β_-^{2nd} and β_-^{3rd}) are shown in this region. The dispersion curve for β_-^{1st} in region 1 ($\varepsilon_{eff} < 0$) rises and asymptotically approaches infinity at $f_4 = 36.31$GHz. Between f_1 and f_5, only β_+^{1st} exists and therefore an opportunity for an isolator at sub-millimeter wavelength could be considered.

V. Conclusion

Two new nonreciprocal waveguiding structures—a grounded dielectric slab with a semiconducting top layer and a grounded semiconductor slab with a dielectric top layer—have been proposed and their dispersion diagrams computed. The results of an analytical and numerical investigation demonstrate that nonreciprocal behavior can be observed in the millimetric and sub-millimetric wavelength regions and that prospects for design of phase shifters and isolators are encouraging. The materials used in this modeling are a low loss dielectric and a (*n*-type) GaAs cooled at liquid nitrogen temperature (77K). Surface plasmon behavior was observed in both forward and reverse wave for both structures and field distributions showing the field displacement effects were also demonstrated. The effects of varying the parameters (e.g. ε_d, B_0) have also been explored and different types of semiconductor, but the results have not been included here for lack of space.

References

[1] J. J. Brion, and R. F. Wallis, "Theory of surface magnetoplasmons in semiconductors," *Phys. Rev. Lett.*, vol. 28, no. 22, pp. 1455-1458, May 1972.

[2] B. G. Martin, A. A. Maradudin, and R. F. Wallis, "Theory of damped surface magnetoplasmons in *n*-type InSb," *Surf. Sci.*, vol. 77, pp. 416-426, 1978.

[3] K. W. Chiu, and J. J. Quinn, "Magnetoplasma surface waves in polar semiconductor: Retardation effects," *Phys. Rev. Lett.*, vol. 29, no. 9, pp. 600-603, August 1972.

[4] N. Marschall, and B. Fischer, "Dispersion of surface polaritons in GaP," *Phys. Rev. Lett.* vol. 28, no. 13, pp. 811-813, March 1972.

[5] S. H. Talisa, and D. M. Bolle, "Performance characteristics of magnetoplasmon based submillimeter wave nonreciprocal devices", *IEEE MTT-S Int. Microwave Symp. Dig.*, vol. 1, pp. 287-289, 1981.

[6] D. M. Bolle, and S. H. Talisa, "Fundamental considerations in millimeter and near-millimeter component design employing magnetoplasmons," *IEEE Trans. Microwave Theory and Tech.*, vol. MTT-29, no. 9, pp. 916-923, September 1981.

[7] S. M. Sze, *Physics of semiconductor devices*, 2nd ed. New York: Wiley Interscience, 1981.

[8] B. Lax, "Magnetoplasma effects in solids," *IRE Trans. Microwave Theory Tech.*, vol. MTT-9, pp. 83-89, January 1961.

[9] C. K. Yong, R. Sloan, and L. E. Davis, "A *Ka*-Band indium-antimonide junction circulator," *IEEE Trans. Microwave Theory and Tech.*, vol. 49, no. 6, pp. 1101-1106, June 2001.

[10] S. Weisbaum, and H. Seidel "The field displacement isolator," *Bell Syst. Tech. Jour.*, vol. 35, pp. 877-898, July 1956.